Available online at www.sciencedirect.com

ScienceDirect

Energy Procedia 80 (2015) 312 – 320

Energy Procedia

12th Deep Sea Offshore Wind R&D Conference, EERA DeepWind'2015

Effect of Turbulence Intensity on the Performance of an Offshore Vertical Axis Wind Turbine

M.Salman Siddiqui[a,*], Adil Rasheed[b], Trond Kvamsdal[a], Mandar Tabib[b]

[a]*Norwegian University of Science and Technology, Department of Mathematical Sciences, Alfred Getz vei 1, 7491 Trondheim, Norway*
[b]*SINTEF ICT, Department of Applied Mathematics, 7465 Trondheim, Norway*

Abstract

Offshore wind energy is one of the most competitive renewable energy resources available to us, which until now been under-exploited. Most of the problems associated with wind farm installation like land acquisition, low wind conditions and its visual impact can be eliminated to large extent by going offshore. In fact it is expected that by the year 2020, 40GW of offshore wind power capacity will be in operation. In an offshore context the wind turbine design methodologies have to address new challenges. For optimal performance the turbine needs to be huge in size and for horizontal axis wind turbines (HAWT) the diameter has already reached a size of 200m. Till now little attention has been paid to vertical axis offshore wind turbines. However, within the NOWITECH project new concepts for vertical axis turbine have been proposed and it might not take a long time before such turbines may become an realistic alternative for use offshore. The current work characterizes variable turbulence intensity flow field around a rotating vertical axis wind turbine (VAWT) in an offshore context. Complete three dimensional numerical transient simulations are performed accounting for the variation of multiple turbulence intensity levels associated with the oncoming wind. Usually offshore winds are highly turbulent in nature partially because of the rapid changes in wind directions along with the sea-air interaction. The results from the study indicate that due to the increase in the turbulence intensity level of 5% to 25% the performance of wind turbine decreases by almost 23% to 42% compared to no turbulence in the incoming wind field.

Peer-review under responsibility of SINTEF Energi AS
Keywords: Wind Energy, Vertical Axis Wind Turbine, Computational Fluid Dynamics, Variable Turbulence Intensity

1. Introduction

With the increase in the demand for more sustainable global energy, wind energy is emerging as one of the most economical alternative in comparison to the rest of renewable energy resources. At first, wind energy installation gained attention in an onshore context only. Large horizontal axis wind turbines (HAWTs) has been designed and integrated to develop wind farms able to produce MW's of energy. However due to low wind speeds, small number of potential wind sites and visual impacts on land, offshore wind industry now experience rapid growth. Recently, the installation of huge wind power plants in the North Sea and the Baltic Sea opens possibilities for the power

* Corresponding author. Tel.: +47-48628035
E-mail address: muhammad.siddiqui@math.ntnu.no, adil.rasheed@sintef.no, trond.kvamsdal@math.ntnu.no, mandar.tabib@sintef.no

Peer-review under responsibility of SINTEF Energi AS
doi:10.1016/j.egypro.2015.11.435

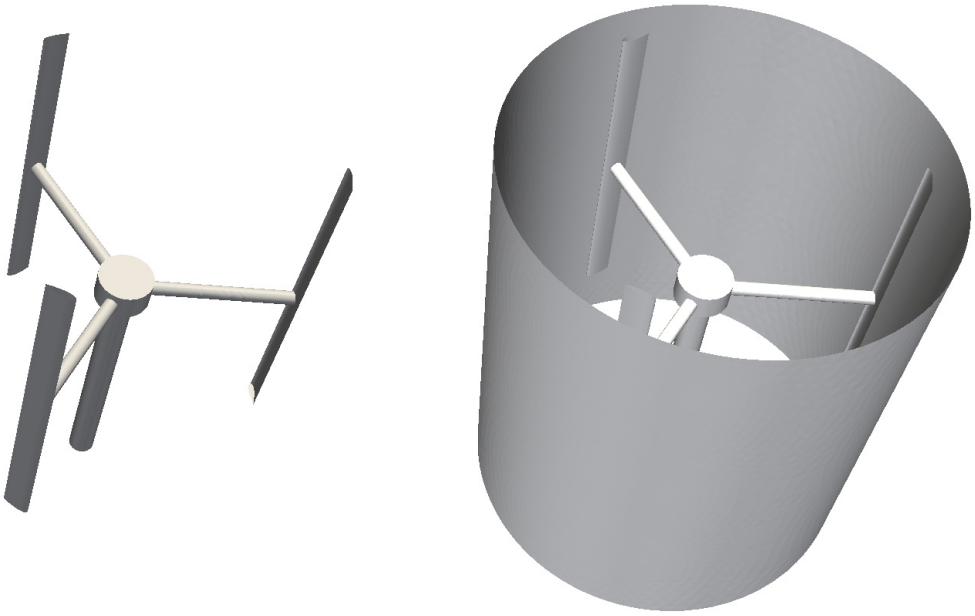

(a) H-type VAWT (Diameter = 2.5m, Chord = 0.2m) (b) Sliding zone surrounding VAWT (Diameter = 3m)

Fig. 1: **H-type VAWT**: Overview of H-type vertical axis wind turbine (VAWT)

production and development of offshore wind turbines. Presently, the cost associated with the installation of offshore wind turbines is higher than installations onshore, and this is considered to be an obstacle for increased investment in offshore wind energy. One important step to overcome this is to design more reliable and efficient turbines for offshore use. Recently, new turbine designs are being introduced to address this issue. Along with horizontal axis wind turbines, new design of vertical axis wind turbine (VAWT) have also emerged, see [1]. One such type of wind turbine that recently has gained popularity is the H-type VAWT, see e.g. [2] and [3]. It has straight blades that can harvest the energy from the wind regardless of the wind direction. This unique feature reduces major costs associated with the traditional HAWT that needs to be aligned with the incoming wind. The H-type VAWT is also considered to be ideal for installations where wind conditions are not consistent i.e. turbulent wind conditions.

The overall objective of this study is to investigate how the performance of vertical axis wind turbine (VAWT) is altered with the change in the turbulence intensity of the incoming flow field. The study covers the expected variations of the wind field that offshore wind turbines will be exposed to. Results are presented in time domain to predict the impact on turbine efficiency in terms of overall torque and power coefficients. The idea is to quantify the performance parameters with varying inflow conditions. Variable flows offer multiple challenges in analyzing aerodynamic and structural behavior of wind turbine. Thus, solid understanding of the flow physics is needed to reduce the risks and increase the performance of wind turbines. Moreover, it also help in the fatigue assessment of the support structures to develop new classes of materials which may further improve the offshore wind turbine technology.

The study herein is a continuation of previous related work by the authors in the field of wind energy modeling. See e.g. [4], [5] and [6] for previous work related to VAWTs, whereas the papers [7] and [8] gives an overview of the work on multi scale modeling for both on-shore and offshore wind turbines and wind farms. Finally, we mention here the work on high Reynolds number aerodynamics of wind turbine blades; see [9], and [10].

2. Methodology

Recently, with access to increased computational power, computational fluid dynamics (CFD) has emerged as a viable option to perform high fidelity simulation predicting the aerodynamic performance of wind turbines. Although CFD-computations may be time consuming and demanding regarding computer resources, the importance of CFD in displaying details of the flow structure should never be underestimated [11].

In this article, CFD-tools are applied to perform high fidelity three dimensional numerical Navier-Stokes simulations of flow around a rotating H-type VAWT. Reynolds averaging is employed, i.e. the flow velocity is split into an average $\overline{\mathbf{u}}$ and a fluctuating part $\mathbf{u}^{'}$, see [6], where we have the following time-filtering of the flow field $\mathbf{u}$:

$$\overline{\mathbf{u}} = \frac{1}{T}\int_T \mathbf{u}(t)dt \tag{1}$$

$$\mathbf{u}^{'} = \mathbf{u} - \overline{\mathbf{u}} \tag{2}$$

The corresponding *steady state* Reynolds Averaged Navier Stokes (RANS) equations reads:

$$\frac{\partial \overline{u_i}}{\partial x_i} = 0 \tag{3}$$

$$\overline{u}_j \frac{\partial u_i}{\partial x_j} = -\frac{1}{\rho}\frac{\partial \overline{p}}{\partial x_i} + \nu \frac{\partial^2 \overline{u_i}}{\partial x_j^2} - \overline{u^{'}_j \frac{\partial u^{'}_i}{\partial x_j}} \tag{4}$$

We first find a steady state solution by solving the Equation (3) and (4). This steady state solution forms the initial condition for our Unsteady Reynolds Average Navier Stokes (URANS) equations displayed in Equation (5) and (6) below. The two-stage procedure simplifies the initial calculations and enables faster convergence in the transient case.

$$\frac{\partial \overline{u_i}}{\partial x_i} = 0 \tag{5}$$

$$\frac{\partial \overline{u_i}}{\partial t} + \overline{u}_j \frac{\partial u_i}{\partial x_j} = -\frac{1}{\rho}\frac{\partial \overline{p}}{\partial x_i} + \nu \frac{\partial^2 \overline{u_i}}{\partial x_j^2} - \overline{u^{'}_j \frac{\partial u^{'}_i}{\partial x_j}} \tag{6}$$

The only difference between the RANS and URANS is addition of the time-derivative (i.e. *unsteady term*) of the velocity on the left hand side in Equation (6) compared to Equation (4). For details of the numerical modeling techniques the reader is referred to e.g. [12] and [13].

The performance of the H-type VAWT is herein assessed for four cases having variable turbulence intensity levels. The turbulence intensity I is defined by the ratio of the vector norm of the fluctuating part ($u^{'}$) and the average of the mean velocity (U), as defined in Equation (7), (8) and (9), respectively.

$$I = \frac{u^{'}}{U} \tag{7}$$

$$u^{'} = \sqrt{\frac{1}{3}(u_x^{'2} + u_y^{'2} + u_z^{'2})} \tag{8}$$

$$U = \sqrt{(\overline{u}_x^2 + \overline{u}_y^2 + \overline{u}_z^2)} \tag{9}$$

Laminar: At first the turbine performance is simulated for the laminar (ideal) case. The inflow wind field is assumed to remain completely horizontally aligned with no disruption between the layers. There are no cross wind parallel to the axis of rotation. There are also no fluctuating components, i.e. the flow field velocity is fully represented by the mean velocity. The resulting torque is expected to be at is maximum as there are no disturbance in the load on the turbine due to fluctuating components of wind velocity.

Low-turbulence intensity (5%): Next the effect of turbulence is simulated and the turbulence intensity are defined by the Equations (7 - (9). The turbulence levels are increased by 5% only. Now the flow field is composed of a mean and fluctuating component. The peak values of the vector norm of the fluctuating components $u^{'}$ remains within the limits of 5% compared to the vector norm of the total velocity field u. In general, this is the average turbulence intensity levels for which offshore wind turbines normally operates.

Medium turbulence intensity (15%): Turbulence intensity is in this case set to 15%. Now the flow field is more chaotic and irregular. The torque is expected to decrease even more in comparison to the laminar case and one may expect increased structural vibrations of the turbine.

High turbulence Intensity (25%): These types of incoming flow regimes are expected in gust and storms. These highly disturbed flow fields are expected to results in lower torques and higher degradation of the turbine blades and the support structure.

3. Computational model

Computational mesh: A CAD-model of the turbine is generated using the CAD-modeler PTC Creo Parameteric and its dimensions are characterized by the rotor diameter 2.5m, and chord length of $C = 0.2$m and the aspect ratio (blade length divided by the chord length) of 12.5, see Figure 1). The fluid domain (hexahedral box with dimension $(50C, 30C, 15.5C)$, where C is the chord length)is discretized by use of tetrahedral elements generated by the mesh generator Gambit. To handle the rotating impeller we use the sliding mesh approach, i.e. the fluid domain is divided into two parts; the outer domain and the inner rotor zone. This will allow the turbine to rotate during the time varying fluid flow computation. In order to adequately capture the flow physics, i.e. boundary layers near solid objects, the tetrahedral fluid mesh is highly refined near the blades, struts, central disc and hub, see Figure 2). The fluid mesh used in our study had $N_{\mathrm{el}} = 2265963$ number of tetrahedral elements and $N_{\mathrm{nod}} = 535171$ number of nodes.

Boundary conditions: In this study we have been using the CFD code Fluent [14] and it has certain acronymes for different boundary conditions. The inflow condition is specified in Fluent as *Velocity inlet*, i.e. in our case the mean velocity was set to $(\overline{u}_x, \overline{u}_y, \overline{u}_z) = (12, 0, 0)$ m/s. The boundary condition at the downwind end of the computational fluid domain is specified in Fluent as *Outflow*, i.e. zero pressure ($p = 0$). The upper and lower domain boundary surfaces are specified as *Far-field*, i.e. the same flow velocities as specified at the inflow. The rotor zone includes the blades, struts and central hub which rotates during the transient solution, thus sliding mesh capability is used and assigned by the command *Interface* boundary condition. There are different types of sliding interface formulation proposed in the literature, for more details the reader is referred to [15]. We have chosen the so called *density based* option in Fluent as studies on dynamic sliding mesh techniques has shown diverging results for the *pressure based* option [16].

Navier-Stokes solver and turbulence model: Second order accurate *Finite Volume Method (FVM)* spatial discretization is employed together with (explicit) *Forward Euler* time integration. The local Reynolds number for each blade given by the relative velocity and the chord length was in our study $70000 \leq R_{\mathrm{e}} \leq 400000$. To handle this high Reynolds flow we chose the $k - \epsilon$ model denoted *Reliazible* in Fluent. A standard wall function is employed for the turbulence model. With our mesh density in the boundary layers the non-dimensional wall distance (in Fluent denoted *Wall YPlus*) to the first layers of nodes (not on the boundary) was up to $y^+ = 50$. The details of the turbulence models, the Navier-Stokes solver [2] and boundary conditions can be found in the ANSYS Fluent User Manual [14].

The numerical simulation was initialized by the values of the inlet boundary throughout the fluid domain. The chosen convergence criterion was specified so that the residuals decrease to 10^{-6} for all the governing equations [5].

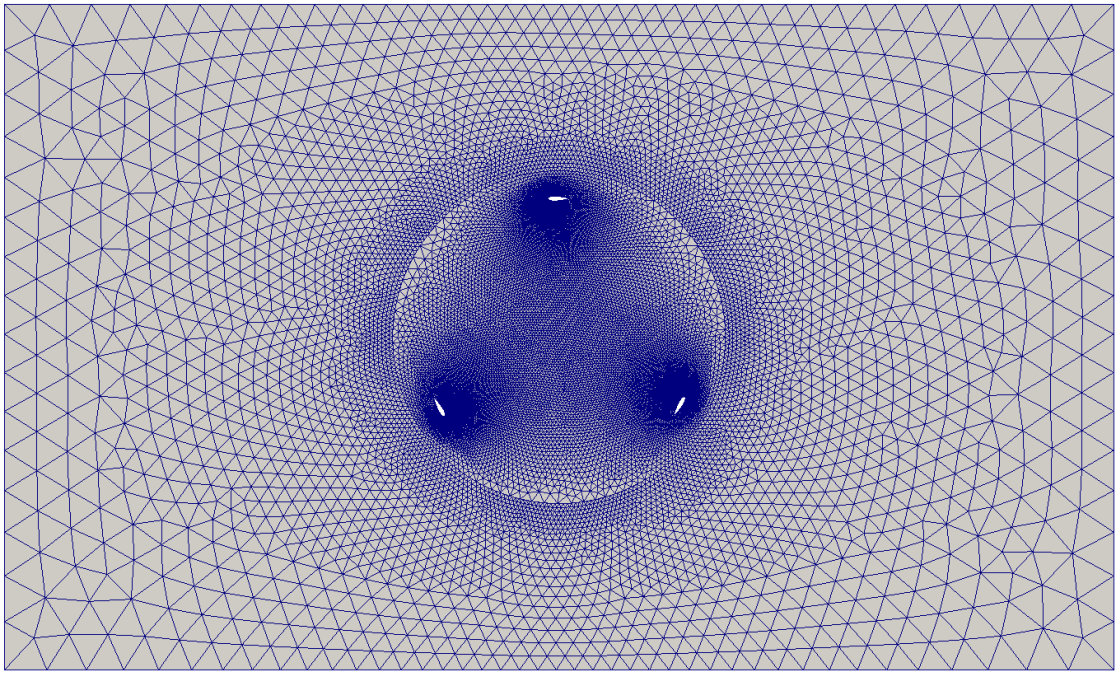

(a) The complete cross section of the tetrahedral mesh

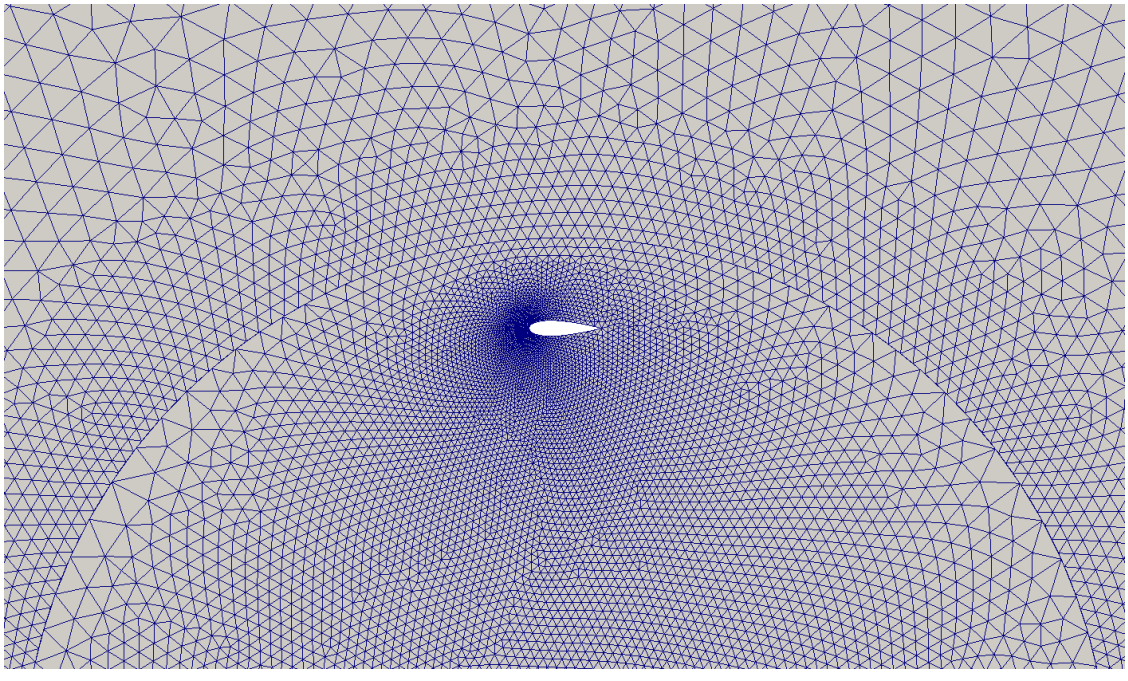

(b) Zoomed-in view of tetrahedral mesh near a blade

Fig. 2: **H-type VAWT**: Two dimensional horizontal cross sections of the tetrahedral CFD-mesh

Sensitivy testing of computational model: For high Reynolds flow problems, like here, one always have to test the sensitivity in the quantity of interest to choice of computational model. Herein, we investigated the sensitivity to choice of domain size, mesh resolution, time step, and different versions of the turbulence model.

We did simplified 2D analysis using different domain sizes: (100C, 50C), (75C, 40C), (50C, 30C) and (40C, 25C) (C is the Chord length) and found that no significant differences in the computed torque for domain sizes equal to and larger than (50C,30C), i.e. we chose this domain size in the horizontal plane [4].

For the mesh resolution we tested three different mesh sizes in 3D: $N_{\text{el}} = \{1.4, 2.2, 3.3\} \cdot 10^6$ and decided to use the medium sized grid.

We tested four different time step sizes $\delta t_{\min} = 0.0001$ and $\delta t_{\max} = 0.0006$, and based on the resulting torques, we decided to use $\delta t = 0.0005$.

Regarding the sensitivity to turbulence model we checked the three different version of $k - \epsilon$ in Fluent denoted *Standard, RNG* and *Realizable*. Both the $k - \epsilon$ RNG and Realizable gave reasonable values of turbulent kinetic energy at the leading edge. However $k - \epsilon$ *Standard* was over-predicting the turbulence values, which is a known anomaly. We decided to use the $k - \epsilon$ *Realizable* together with standard wall function [1].

4. Results and discussions

4.1. Turbine performance under varying turbulence intensity

RANS CFD-simulations provides useful estimate of power output and blade loads for different design configurations [1]. For a VAWT, at any given time, the rotating blades at downstream rear-end gets subjected to a passing turbulent flow-field (that is generated earlier by rotating blades at upstream). This can influence overall performance of a VAWT. The results of the RANS based simulations are shown in the Figure 3. It shows the vorticity at horizontal planes along different span wise direction indicating the turbulence generated by the upwind blades. It is also seen that the flow field is turbulent in the upwind path ($0^o - 180^o$). The interaction of the incoming flow and the rotating turbine results in large blade tip vortices. These rotational disturbances once generated from the blade-tip in the upwind path, travels to the downwind side. The blade-tip swirls from upwind to the downwind side, causing the downwind blades to pass through increased turbulence generated from the upwind side. In addition the flow also gets obstructed due to the central shaft disc and support arms. These flow interactions further reduce the power resulting in drop in torque ripple values during the rotation.

4.2. Numerical investigation under varying turbulent intensity

The performance parameter, quantity of interest, selected in this study is the generated torque. In Figure 4 the torque ripple over four cycles are displayed for the four different cases with various turbulence intensity levels. The data for these four cycles are taken after seven cycles when the fluctuations in the flow field settles down. Notice that it is the torque generated by a **single blade** during the complete rotation of the turbine. The blade extracts maximum amount of torque during its upwind path ($0^o - 180^o$) as compared to its downwind path ($180^o - 360^o$). This is because the blade extracts the energy from the wind and shed vortices's in the upwind path. As the blade pass through downwind path, its performance is affected by the wakes and low wind speed which cause reduction in power outputs. We observe that the maximum value for the case with no turbulence intensity in the inflow is about 130 kN, whereas the same result for the case with 25% turbulence intensity is around 100 kN.

In Figure 5 we show the torque ripples for the four cases with variying turbulence intensity, taken as the average of the four cycles shown in Figure 4. Here, we again see the difference in maximum torque around 90^o, but also the difference between the no turbulent incoming flow and the turbulent incoming flow downwind path ($180^o - 360^o$).

Regarding power production we are interested in the average torque per cycle, therefore we have in Table 1 shown the average torque for the four different cases with different turbulence intensity in the incoming flow. From Table 1 we see a significant drop, i.e. 23%, in average torque even for the case with 5% turbulence intensity and as much as 42% for the case with 25% turbulence intensity.

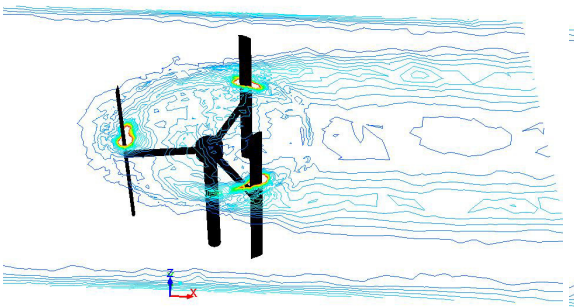

(a) Vorticity due to blades only (z = 2.5 m)

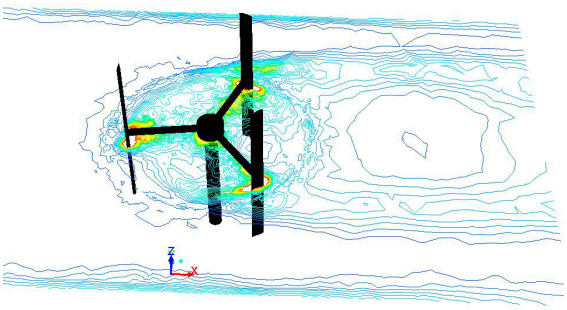

(b) Vorticity due to blades and cylinder (z = 1.9 m)

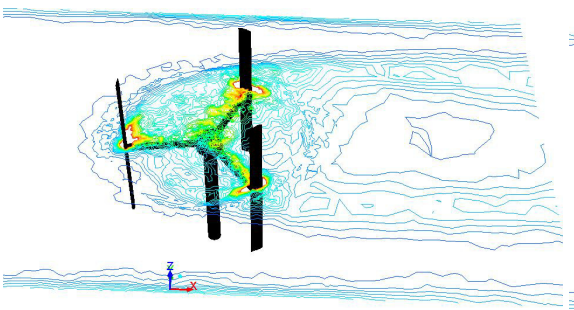

(c) Vorticity due to blades and central disc (z = 2.1 m)

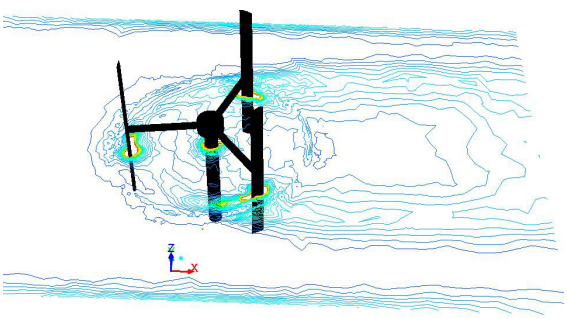

(d) Vorticity due to blades and lower cylinder (z = 1.5 m)

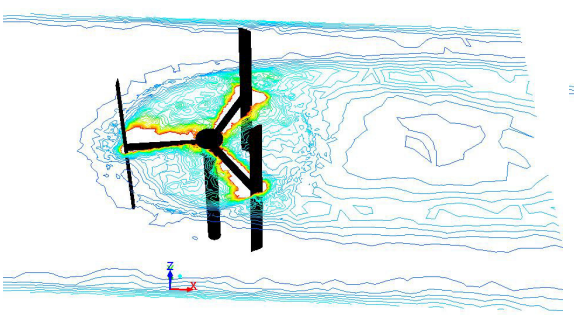

(e) Vorticity due to blades, disc and struts (z = 2.0 m)

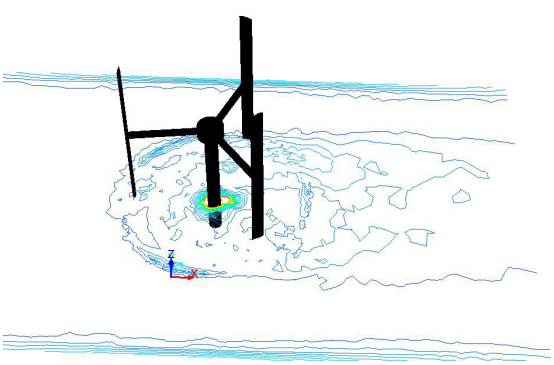

(f) Vorticity due to cylinder only(z = 0.5 m)

Fig. 3: **H-type VAWT**: Vorticity contours at different horizontal planes

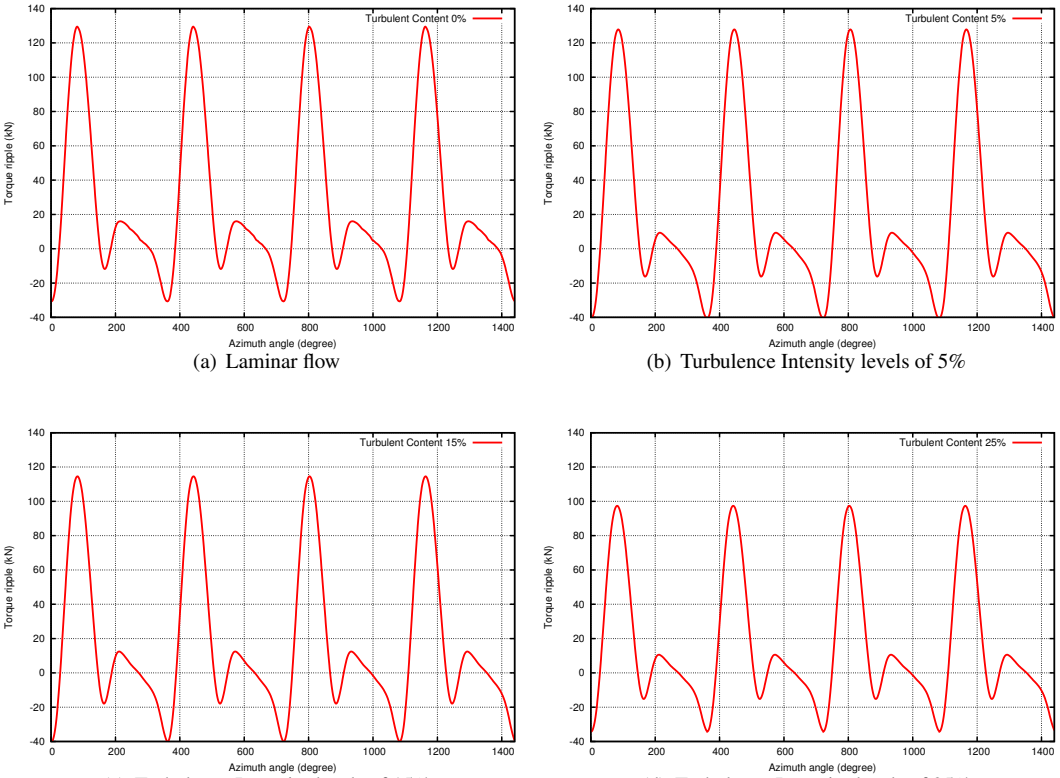

(a) Laminar flow (b) Turbulence Intensity levels of 5%

(c) Turbulence Intensity levels of 15% (d) Turbulence Intensity levels of 25%

Fig. 4: **H-type VAWT**: Torque ripple over four cycles

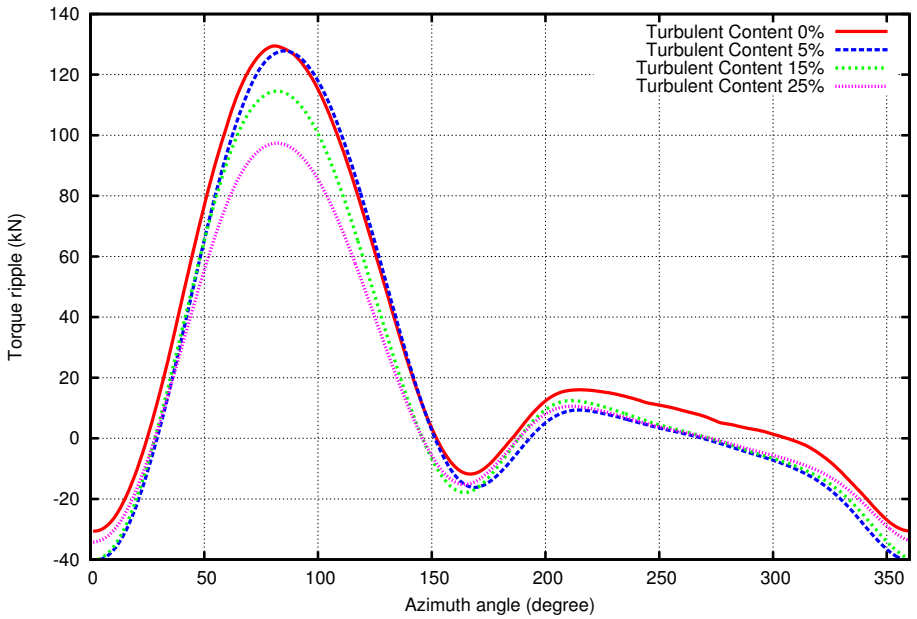

Fig. 5: **H-type VAWT**: Comparison of torque ripple under varying turbulent intensity

Table 1: **H-type VAWT**: Percentage drop in Average Torque in terms of turbulence intensity

S.No	Turbulence Content	Average Torque	Drop in Average Torque
Case I	0%	25.86	0%
Case II	5%	19.72	23%
Case III	15%	17.16	33%
Case IV	25%	14.80	42%

5. Conclusions

The very essence of a wind turbine is to convert kinetic energy in the wind field to mechanical energy (through torque) and then to electrical energy. Thus, a given turbine designs ability to generate large torque during operation is an important performance indicator. Herein, we have studied the influence of turbulence intensity in the incoming flow field on the generation of torque for a H-type VAWT. As the torque varies significantly during the rotation of the VAWTs impeller we have focused on the average torque per cycle. In our numerical study we investigated the effect for turbulent intensity levels of 0%, 5%, 15% and 25% in the incoming flow field. The results shows that the average torque over an cycle decreases by almost 23%, 33% and 42% compared to no turbulent flow, respectively. A reduction in toque is expected as having turbulent inflow conditions may be compared to the wind turbine being in the wake downstream another wind turbine. However, the size of the reduction has up to now not been studied in detail for H-type VAWT, and we think that our study is an interesting contribution in this regard.

References

[1] Bhutta, M.M.A., Hayat, N., Farooq, A.U., Ali, Z., Jamil, S.R., Hussain, Z.. Vertical axis wind turbine – a review of various configurations and design techniques. Renewable and Sustainable Energy Reviews 2012;16(4):1926 – 1939.

[2] Eriksson, S., Bernhoff, H., Leijon, M.. Evaluation of different turbine concepts for wind power. Renewable and Sustainable Energy Reviews 2008;12(5):1419 – 1434.

[3] Brusca, S., Lanzafame, R., Messina, M.. Design of a vertical-axis wind turbine: how the aspect ratio affects the turbines performance. International Journal of Energy and Environmental Engineering 2014;5(4):333–340.

[4] Siddiqui, M.S., Durrani, N., Akhtar, I.. Numerical study to quantify the effects of struts and central hub on the performance of a three dimensional vertical axis wind turbine using sliding mesh. In: ASME 2013 Power Conference. American Society of Mechanical Engineers; 2013, p. V002T09A020.

[5] Khalid, M.S.U., Rabbani, T., Akhtar, I., Durrani, N., Siddiqui, M.S.. Reduced-order modeling of torque on a vertical-axis wind turbine at varying tip speed ratios. Journal of Computational and Nonlinear Dynamics 2015;10(4):041012.

[6] Siddiqui, M.S., Durrani, N., Akhtar, I.. Quantification of the effects of geometric approximations on the performance of a vertical axis wind turbine. Renewable Energy 2015;74:661 – 670.

[7] Rasheed, A., Sørli, K., Holdahl, R., Kvamsdal, T.. A multiscale approach to micrositing of wind turbines. Energy Procedia 2012;14:1458 – 1463.

[8] Rasheed, A., Holdahl, R., Kvamsdal, T., Åkervik, E.. A comprehensive simulation methodology for fluid-structure interaction of offshore wind turbines. Energy Procedia 2014;53:135 – 145.

[9] Nordanger, K., Holdahl, R., Kvarving, A.M., Rasheed, A., Kvamsdal, T.. Implementation and comparison of three isogeometric navier–stokes solvers applied to simulation of flow past a fixed 2d naca0012 airfoil at high reynolds number. Computer Methods in Applied Mechanics and Engineering 2015;284:664–688.

[10] Nordanger, K., Holdahl, R., Kvamsdal, T., Kvarving, A.M., Rasheed, A.. Simulation of airflow past a 2d naca0015 airfoil using an isogeometric incompressible navier–stokes solver with the spalart–allmaras turbulence model. Computer Methods in Applied Mechanics and Engineering 2015;290:183–208.

[11] Johansen, J., Sørensen, N.. Aerofoil characteristics from 3D CFD rotor computations. Wind Energy 2004;7(4):283–294.

[12] Versteeg, H.K., Malalasekerah, W.. An Introduction to Computational Fluid Dynamics: The Finite Volume Method. Harlow, Pearson Education Limited; 2007.

[13] Tu, J.Y., Yeoh, G.H., Liu, C.Q.. Computational Fluid Dynamics: A Practical Approach. Oxford, Butterworth-Heinemann; 2008.

[14] Fluent, . Fluent User's Manual. ANSYS; 2010.

[15] Bazilevs, Y., Korobenko, A., Deng, X., Yan, J.. Novel structural modeling and mesh moving techniques for advanced fluidstructure interaction simulation of wind turbines. International Journal for Numerical Methods in Engineering 2015;102(3-4):766–783.

[16] Hwang, I., Min, S., Jeong, I., Lee, Y., Kim, S.. Efficiency Improvement of anew Vertical Axis Wind Turbine by Individual Active Control of Blade Motion. School of Mechanical and Aerospace Engineering, Seoul National University, The Republic of Korea; 2006.